Atmos. Meas. Tech. Discuss., 5, 4473–4494, 2012
www.atmos-meas-tech-discuss.net/5/4473/2012/
doi:10.5194/amtd-5-4473-2012

Atmospheric Measurement Techniques Discussions

On the efficient treatment of temperature profiles for the estimation of atmospheric transmittance under scattering conditions

R. Lindstrot and R. Preusker

Institut für Weltraumwissenschaften, Freie Universität Berlin, Carl-Heinrich-Becker-Weg 6–10, 12165 Berlin, Germany

Received: 20 April 2012 – Accepted: 14 June 2012 – Published: 29 June 2012

Correspondence to: R. Lindstrot (rasmus.lindstrot@wew.fu-berlin.de)

Published by Copernicus Publications on behalf of the European Geosciences Union.

Abstract

The vertical temperature profile in the atmosphere influences the top-of-atmosphere radiance in regions of atmospheric absorption bands. In the visible and near infrared part of the spectrum, this poses a problem for the fast forward simulation of the radiative transfer, needed in algorithms for the retrieval of any atmospheric or surface-related parameter. We show that the main part of the global variability of temperature profiles can be described by their first 2 to 6 eigenvectors, depending on the accuracy requirement, by performing a Principal Component Analysis (PCA) on a global set of temperature profiles from the Global Forecast System (GFS). Furthermore, we demonstrate the possibility to approximate the atmospheric transmittance in the oxygen A band for any temperature profile with almost perfect accuracy by a linear combination of the transmittances attributed to each of the significant temperature eigenvectors. For the retrieval of surface pressure from oxygen A band measurements, this reduces the global root mean square error from >30 hPa to better than 1 hPa by strongly reducing the regional bias of surface pressure, retrieved on the assumption of an average temperature profile. The technique can be applied under scattering conditions, to eliminate any temperature-induced errors in e.g. simulated radiances. Generally, the method can be applied to any problem including gaseous absorption or emission, such as e.g. the retrieval of water vapour content or sea surface temperature.

1 Introduction

The efficient forward simulation of the radiative transfer in the atmosphere is an essential component of any remote sensing algorithm for the retrieval of atmospheric or surface-related parameters. Especially if both gaseous absorption and scattering from molecules or aerosols in the atmosphere are important, such as in gaseous absorption bands in the visible and near infared part of the electromagnetic spectrum, the requirements regarding the speed of the forward simulation are impossible to meet

AMTD
5, 4473–4494, 2012

with state-of-the-art computers, no matter which radiative transfer code is used. Consequently, many forward simulation modules employed in retrieval algorithms in the shortwave region are based on pre-calculated look-up tables of the desired radiative quantity, which is tabulated as a function of e.g. the measurement geometry and any influencing geophysical parameter (see, e.g. Gao and Kaufman, 2003; Lindstrot et al., 2012). Within absorption bands, the measurement is influenced by the vertical temperature profile through the pressure- and temperature-dependent line broadening mechanisms (e.g. Liou, 2002). The Doppler frequency shift caused by the molecular velocities results in a temperature-dependent line width, described by the Doppler line shape:

$$f_{\mathrm{D}}(\nu - \nu_0) = \frac{1}{\alpha_{\mathrm{D}}\sqrt{\pi}} \exp\left[\frac{(\nu - \nu_0)^2}{\alpha_{\mathrm{D}}^2}\right]$$

with the Doppler line width $\alpha_{\mathrm{D}} \propto T^{1/2}$. Additionally, absorption lines are broadened by molecular collisions, described by the Lorentz line shape:

$$f_{\mathrm{L}}(\nu - \nu_0) = \alpha_{\mathrm{L}}/\pi/((\nu - \nu_0)^2 + \alpha_{\mathrm{L}}^2)$$

with the Lorentz line width α_{L}, which is roughly proportional to the number of collisions per unit time: $\alpha_{\mathrm{L}} \propto pT^{-1/2}$.

The resulting line can approximately be described by the Voigt line shape, which is obtained from a convolution of both line profiles. In the lower atmosphere, the dominant process is pressure broadening with the resulting inverse influence of the temperature on the line width. An absorption line will therefore be broadened with increasing pressure and decreasing temperature, in case the whole vertical column of the atmosphere is traversed.

It is not feasible to tabulate the simulated quantity as a function of the temperature in each vertical atmospheric layer, since this would result in look-up tables with an excessive, non-manageable number of dimensions. It is indeed not necessary, since the individual layer temperatures are highly correlated and can be described with a much

AMTD
5, 4473–4494, 2012

lower number of parameters, such as determined by means of a Principal Component Analysis.

The reconstruction of globally occurring temperature profiles is possible on the basis of a few eigenvectors, as demonstrated in Sect. 2.1. Furthermore, the atmospheric transmittance for an arbitrary temperature profile can be approximated in a similar way, as proposed in Sect. 2.2. This is demonstrated by applying the method to the retrieval of surface pressure from oxygen A band measurements (see Sect. 3). The applicability for the correction of radiances is demonstrated in Sect. 3.2.

2 Statistical analysis

2.1 PCA of global temperature profiles

The natural variability of the temperature profile was analyzed using data of the Global Forecast System (GFS), providing the temperature on 26 pressure levels at a $1 \times 1^{\circ}$ resolution. A single, global field of temperature profiles from 19 October 2007 was used for the analysis. All following studies and plots are based on this case.

Due to the high correlation of the temperature among neighbouring vertical layers, the number of independent parameters that suffice to reconstruct each vertical profile is significantly smaller than the number of pressure levels. A suitable statistical tool to reduce the dimensionality of a data set is a Principal Component Analysis (PCA, see, e.g. Peixoto and Oort, 1992), a technique frequently used in various fields including atmospheric modeling and remote sensing (see, e.g. Natraj et al., 2005). A PCA was performed on a global field of temperature profiles, revealing that e.g. the three most significant eigenvectors v_i are sufficient to reproduce 96 % of the variability inherent to the data (see Table 1).

AMTD
5, 4473–4494, 2012

A random temperature profile T can be expressed as the sum of the average profile T_{mean} and a linear combination of the significant eigenvectors v_i:

$$T = T_{\text{mean}} + \sum_{i=0}^{\text{ncomp}} c_i v_i \quad (1)$$

where ncomp is the number of eigenvectors used. The weight c_i of each eigenvector is obtained from $c_i = (T - T_{\text{mean}})\#v_i$ (# denotes a matrix multiplication). Figure 1 shows three arbitrary profiles as extracted from GFS data and their reconstruction, using the three most significant eigenvectors. While the dashed red curve shows an almost perfect representation of the vertical temperature profile, the green case reveals that more eigenvectors are needed to reconstruct the vertical fine structure, e.g. in cases of boundary layer temperature inversions. The blue case, representing an arctic atmosphere, shows that an extremely low tropopause height results in some deviations of the reconstructed profile. However, since the goal here is just to reduce the dimensionality of the problem for the efficient estimation of the atmopsheric transmittance, these secondary deviations between true and reconstructed temperature profile can be regarded as of minor influence.

2.2 Similarity between temperature and transmittance

The strategy pursued in this work is based on the assumption that a similarity between the temperature profile and the atmospheric transmittance exists. This would mean that the transmittance associated with any temperature profile can be constructed by a linear combination of the transmittances associated with the temperature profile eigenvectors, using the same weights c_i as in Eq. (1).

The effect of eigenvector v_i on the atmospheric transmittance can be calculated as

$$\Delta t_{v_i} = t_{\text{mean}} - t_{\text{mean}+v_i} \quad (2)$$

AMTD
5, 4473–4494, 2012

where t_{mean} is the transmittance of the average temperature profile T_{mean}, $t_{\mathrm{mean}+v_i}$ is the transmittance of the average profile, modified by eigenvector v_i, and Δt_{v_i} is the associated difference in transmittance for eigenvector v_i, all for a given airmass.

In accordance with Eqs. (1) and (2), the transmittance t for a random temperature profile T is then constructed by a linear combination of the mean transmittance t_{mean} and the contributions of each eigenvector Δt_{v_i}, using the same weights c_i as determined for the temperature profile eigenvectors:

$$t = t_{\mathrm{mean}} + \sum_{i=0}^{\mathrm{ncomp}} c_i \Delta t_{v_i}. \quad (3)$$

In case the similarity of temperature and transmittance is fulfilled, it would therefore be sufficient to calculate the transmittance t_{mean} and ncomp perturbations to be able to construct the transmittance for any temperature profile. This means a major simplification of the calculation of atmospheric transmittance and enables the inclusion of the temperature profile effect. The validity of the approach is demonstrated in Sect. 3 for the retrieval of surface pressure from measurements in the oxygen A band and the approximation of radiances.

3 Application in the oxygen A band

3.1 Transmittance approximation

In order to test the approach for the approximation of atmospheric transmittance, the global set of GFS temperature profiles was used to calculate the average oxygen A band transmittance $t_{\mathrm{O_2A}}$ between 760 nm and 763 nm for a fixed solar zenith angle of 45° and nadir view, hereby using the HITRAN 2008 database (Rothman et al., 2009). The problem was simplified by assuming a globally constant surface pressure of 1000 hPa, neglecting surface elevation, in order to isolate the effect of temperature

AMTD
5, 4473–4494, 2012

broadening on the oxygen absorption lines (see Fig. 2 for an example of the transmittance in the considered spectral window).

The resulting global transmittance for the considered case is shown in in Fig. 3. The highest transmittance, respectively weakest oxygen absorption, is found in regions with the highest temperatures, namely over tropical land areas. As stated before, this is due to the pressure- and temperature-dependence of the Lorentz line widths, resulting in less broadened absorption lines for higher temperatures.

The hypothetical transmittance for the given airmass of 2.41 varies between 0.227 in the Antarctic and 0.265 in the tropics. For comparison, a transmittance $t^*_{O_2A}$ was obtained by a linear combination of the eigenvector contributions, following Eq. (3).

The global root mean square deviation of the derived transmittance is shown in Fig. 4 as a function of the number of eigenvectors used for the approximation of transmittance. The error is reduced from roughly 1 % of transmittance, in case an average temperature profile is assumed, to 0.09 %, by just using the first temperature profile eigenvector to modify the average transmittance. Adding the second eigenvector yields a further reduction of the transmittance error below 0.05 %. The error can be brought down to 0.015 % by using 6 eigenvectors. The residual 0.015 % are caused by the weak non-linearity between temperature and transmittance. Figure 5 shows the global distribution of the errors of $t^*_{O_2A}$ for the case of using 1, 2, 3 or 4 eigenvectors. In case of using only the most significant eigenvector, some systematic deviations of the approximated transmittance are apparent, with positive biases found mainly over Antarticta and Africa and negative biases found mainly over the extratropical oceans. These systematic biases are gradually eliminated with increasing number of eigenvectors and are almost totally removed in case four or more eigenvectors are used.

As an example, satellite measurements in the oxygen A band can be used for the retrieval of surface pressure, as demonstrated by e.g. Barton and Scott (1986); Mitchell and O'Brien (1987); Breon and Bouffies (1996) and O'Brien et al. (1998). The authors have developed a corresponding algorithm based on such measurements performed by the Medium Resolution Imaging Spectrometer (MERIS) onboard ENVISAT

AMTD
5, 4473–4494, 2012

(Lindstrot et al., 2009), and used it to find empirical coefficients for the correction of instrumental stray light (Lindstrot et al., 2010). However, the initial algorithm version is based on the assumption of a fixed, average temperature profile, resulting in regional surface pressure biases of up to 50 hPa, as shown in Fig. 6, left panel. If the temperature profile variability is accounted for using the technique described above, these large systematic errors can be eliminated, as shown in Fig. 6, right panel. The corresponding global root mean square error of surface pressure due to temperature profile effects is reduced from 35 hPa to less than 0.5 hPa, if six or more eigenvectors are used (see Fig. 7). Since other error sources, such as aerosol scattering or the spectral calibration uncertainty, result in much larger errors in derived surface pressure (Lindstrot et al., 2009), using two eigenvectors to describe the temperature profile variability is sufficient to account for the temperature-dependence of the oxygen absorption.

3.2 Radiance approximation

We suggest to use the technique under scattering conditions to approximate the top-of-atmosphere (TOA) radiances for any given temperature profile from the corresponding TOA radiances associated with each temperature profile eigenvector. By replacing the transmittance t with radiance L, Eq. (3) becomes:

$$L_{\mathrm{ncomp}} = L_{\mathrm{mean}} + \sum_{i=0}^{\mathrm{ncomp}} c_i \Delta L_{v_i}. \quad (4)$$

This means that the radiance for any atmospheric profile, observing geometry and geophysical condition can be represented by a linear combination of the tabulated L_{mean} and ncomp radiances.

In order to test this hypothesis, we have performed full radiative transfer calculations of a MERIS-like medium-spectral-resolution channel within the oxygen A band, using the Matrix Operator Model (MOMO, Fell and Fischer, 2001; Hollstein and Fischer, 2012). The spectral channel was assumed to have a Gaussian shape with a width of

AMTD
5, 4473–4494, 2012

3 nm and shifted through the absorption band to visualize the spectral stability of the approach. In order to isolate the effect of scattering on the accuracy of the method, two general cases were studied:

a. A case with a strong influence of atmospheric scattering, i.e. a high aerosol loading (aerosol optical depth $AOD_{550\,nm} = 0.5$) over dark Lambertian surface (albedo $\alpha = 0.1$).

b. A case with a weaker influence, i.e. a low aerosol loading ($AOD_{550\,nm} = 0.1$), over a bright Lambertian surface ($\alpha = 0.5$).

The approximation of the TOA radiance was performed following Eq. (4) for a tropical and a polar temperature profile with a surface pressure of 1000 hPa (see red and blue profiles in Fig. 1).

Figure 8 shows the angular dependency of the differences found between the TOA radiances simulated using the average temperature profile and the tropical profile, respectively, for both cases and a relative azimuth angle of 0°, i.e. the sensor is placed opposite of the sun. If the average temperature profile is used, the deviation of the TOA radiance from the truth, ΔL_{mean}, is between −4 % (Case A) and −3 % (Case B) for low zenith angles (sensor and sun close to zenith) and rises to −8 % (Case A) and −7 % (Case B) for high angles. Similar numbers with reversed sign are found for the polar case. When the first two eigenvectors are used for correcting the radiance, the error, ΔL_2, is below 1 % for both cases at all viewing geometries. There is no significant influence of the observation geometry on the accuracy of the method, which is able to eliminate the overall bias and its angular dependence.

Figure 9, left panel, shows the influence of the number of eigenvectors on the approximation error as an average over all viewing geometries. For both cases and both profiles, the initial error of several percent is reduced to well below 1 % by using the first temperature eigenvector and slightly improved by accounting for the second eigenvector. The addition of further eigenvectors does not significantly change the result. The elimination of the temperature-induced radiance bias works for both cases with the

AMTD
5, 4473–4494, 2012

same accuracy, proving that for this purpose atmospheric scattering is not a critical issue. The right panel of Fig. 9 shows ΔL_{mean} and ΔL_2 for case A as a function of central wavelength. While ΔL_{mean} shows a strong dependency on the central wavelength with a clear maximum around 762.5 nm, ΔL_2 is spectrally almost constant and close to zero. Since, depending on the instrument construction type, the central wavelengths of spectral channels can vary with time or the view angle (see for instance Delwart et al., 2007), it is important to account for these spectral effects to avoid temporal or view angle dependent biases.

4 Conclusions

We have presented a method to efficiently approximate the effect of the temperature profile on the atmospheric transmittance. The first two to six eigenvectors are sufficient to describe the global variability of temperature profiles, depending on what accuracy is required. The temperature eigenvectors can serve to calculate the corresponding transmittance variations and thus to approximate the atmospheric transmittance for any arbitrary temperature profile. As shown in an exemplary application for the case of oxygen absorption around 0.76 µm, the thus approximated transmittance is in perfect agreement with the truth if a sufficient number of eigenvectors are used. In the shown case, an average oxygen transmittance of 0.25 between 760 nm and 763 nm for an airmass of 2.41 and a surface pressure of 1000 hPa, the residual error of the approximated transmittance was in the range of 0.0015 in absolute transmittance, which is 0.06 %. Depending on the nature of the application, the number of eigenvectors needed may vary. As demonstrated for the retrieval of surface pressure, using two eigenvectors is sufficient since the resulting residual error of 1.5 hPa is much smaller than that of other error sources. The same holds for the retrieval of water vapour column amount from near infrared measurements, since the majority of water vapour molecules are concentrated in the lower atmosphere with a resulting weaker influence of the vertical temperature profile on the absorption lines. The technique can readily be used for the

AMTD
5, 4473–4494, 2012

elimination of any temperature-induced bias in simulated radiances. Within the oxygen A band, using one or two eigenvectors is sufficient. Scattering at molecules and particles does not affect the applicability or accuracy of the method.

The benefit of the presented method can either be seen as

- a major speed up of the calculation of transmittance or radiance in any forward simulation module used to model radiative transfer in atmospheric absorption bands, or
- the avoidance of temperature-induced errors in calculated radiances at the cost of merely doubling or tripling the amount of simulations to be performed.

Acknowledgement. This work was carried out in the frame of the ESA ESTEC-funded project "Atmospheric corrections for fluorescence signal and surface pressure retrieval over land" (contract nr. 4000102733).

References

Barton, I. J. and Scott, J. C.: Remote measurement of surface pressure using absorption in the oxygen A-band, Appl. Optics, 25, 3502–3507, 1986. 4479

Breon, F. M. and Bouffies, S.: Land surface pressure estimate from measurements in the oxygen A absorption band, J. Appl. Meteorol., 35, 69–77, 1996. 4479

Delwart, S., Preusker, R., Bourg, L., Santer, R., Ramon, D., and Fischer, J.: MERIS inflight spectral calibration, J. Appl. Remote Sens., 28, 479–496, 2007. 4482

Fell, F. and Fischer, J.: Numerical simulation of the light field in the atmosphere-ocean system using the matrix-operator method, J. Quant. Spectrosc. Ra., 3, 351–388, 2001. 4480

Gao, B.-C. and Kaufman, Y. J.: Water vapor retrievals using moderate resolution imaging spectroradiometer (MODIS) near-infrared channels, J. Geophys. Res., 108, 4389, doi:10.1029/2002JD003023, 2003. 4475

Hollstein, A. and Fischer, J.: Radiative transfer solutions for coupled atmosphere ocean systems using the matrix operator technique, J. Quant. Spectrosc. Ra., 113, 536–548, doi:10.1016/j.jqsrt.2012.01.010, 2012. 4480

AMTD

5, 4473–4494, 2012

On the efficient treatment of temperature profiles

R. Lindstrot and R. Preusker

Lindstrot, R., Preusker, R., and Fischer, J.: The retrieval of land surface pressure from MERIS measurements in the oxygen A band., J. Atmos. Ocean. Tech., 26, 1367–1377, 2009. 4480
Lindstrot, R., Preusker, R., and Fischer, J.: The empirical correction of stray light in the MERIS oxygen A band channel, J. Atmos. Ocean. Tech., 27, 1185–1194, 2010. 4480
Lindstrot, R., Preusker, R., Diedrich, H., Doppler, L., Bennartz, R., and Fischer, J.: 1D-Var retrieval of daytime total columnar water vapour from MERIS measurements, Atmos. Meas. Tech., 5, 631–646, doi:10.5194/amt-5-631-2012, 2012. 4475
Liou, K.: An Introduction to Atmospheric Radiation, International Geophysics Series, Academic Press, 2002. 4475
Mitchell, R. M. and O'Brien, D. M.: Error estimates for passive satellite measurement of surface pressure using absorption in the A band of oxygen, J. Atmos. Sci., 44, 1981–1990, 1987. 4479
Natraj, V., Jiang, X., Shia, R., Huang, X., Margolis, J. S., and Yung, Y. L.: Application of principal component analysis to high spectral resolution radiative transfer: a case study of the O_2 A band, J. Quant. Spectrosc. Ra., 95, 539–556, doi:10.1016/j.jqsrt.2004.12.024, 2005. 4476
O'Brien, D., Mitchell, R., English, S., and Da Costa, G.: Airborne measurements of air mass from O_2 A-band absorption spectra, J. Atmos. Ocean. Tech., 15, 1272–1286, 1998. 4479
Peixoto, J. and Oort, A.: Physics of Climate, American Institute of Physics, American Institute of Physics Press, Woodbury, NY, USA, 1992. 4476
Rothman, L., Gordon, I., Barbe, A., Benner, D., Bernath, P., Birk, M., Boudon, V., Brown, L., Campargue, A., Champion, J.-P., Chance, K., Coudert, L., Dana, V., Devi, V., Fally, S., Flaud, J.-M., Gamache, R., Goldman, A., Jacquemart, D., Kleiner, I., Lacome, N., Lafferty, W., Mandin, J.-Y., Massie, S., Mikhailenko, S., Miller, C., Moazzen-Ahmadi, N., Naumenko, O., Nikitin, A., Orphal, J., Perevalov, V., Perrin, A., Predoi-Cross, A., Rinsland, C., Rotger, M., Simeckova, M., Smith, M., Sung, K., Tashkun, S., Tennyson, J., Toth, R., Vandaele, A., and Auwera, J. V.: The HITRAN 2008 molecular spectroscopic database, J. Quant. Spectrosc. Ra., 110, 533–572, doi:10.1016/j.jqsrt.2009.02.013, 2009. 4478

AMTD
5, 4473–4494, 2012

Table 1. Eigenvalues and percentage of (cumulative) variance for first 10 eigenvectors.

Eigenvector v_i	Eigenvalue	Percentage of variance	Cumulative percentage of variance
1	3471	82.4 %	82.4 %
2	421	10.0 %	92.4 %
3	162	3.8 %	96.2 %
4	65	1.6 %	97.8 %
5	42	1.0 %	98.8 %
6	14	0.3 %	99.1 %
7	10	0.3 %	99.4 %
8	7	0.1 %	99.5 %
9	4	0.1 %	99.6 %
10	3	0.1 %	99.7 %
...	...	...	...

AMTD
5, 4473–4494, 2012

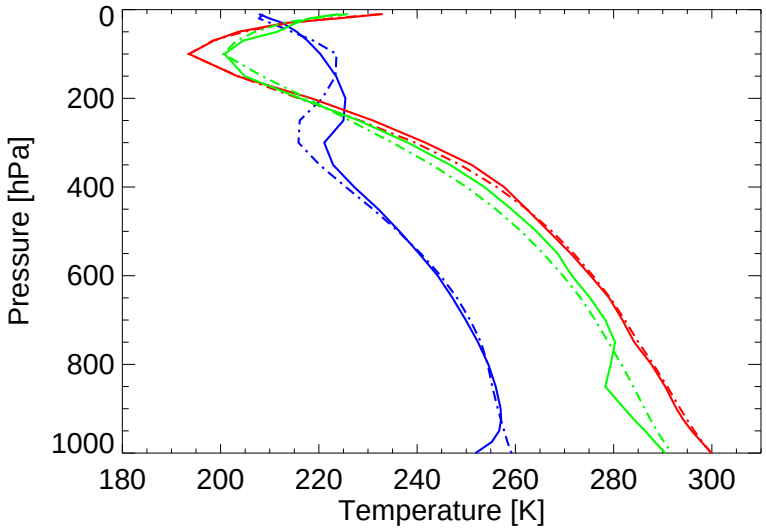

Fig. 1. Three arbitrary temperature profiles (solid lines) and their reconstruction (dashed lines) using the three most significant eigenvectors.

AMTD
5, 4473–4494, 2012

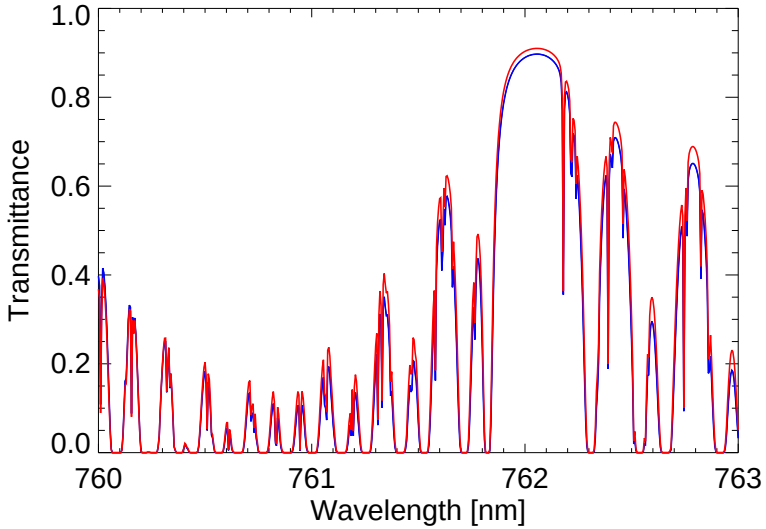

Fig. 2. Atmospheric transmittance in oxygen A band for an arctic (blue) and a tropical temperature profile (red), a surface pressure of 1000 hPa and an airmass of 2.41 (solar zenith of 45°, nadir view).

AMTD
5, 4473–4494, 2012

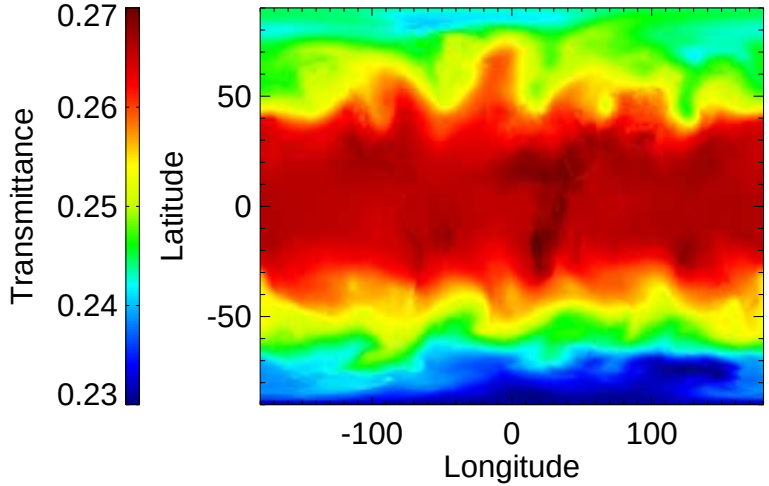

Fig. 3. Global transmittance t_{O_2A} for GFS temperature profiles, a constant surface pressure of 1000 hPa, solar zenith angle of 45° and nadir view.

AMTD
5, 4473–4494, 2012

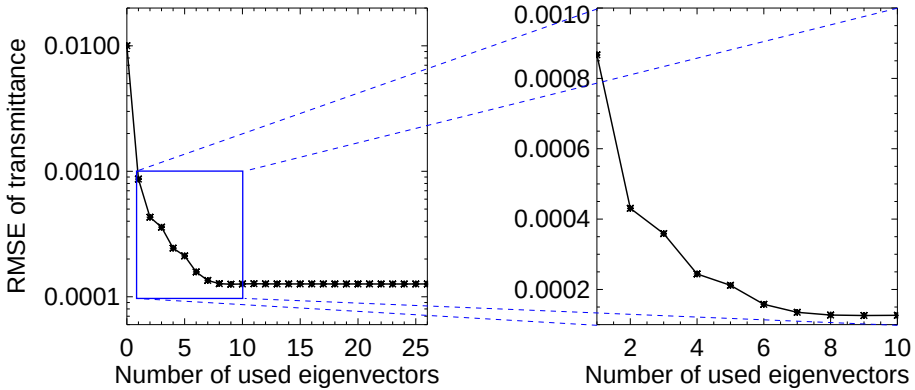

Fig. 4. Global root mean square error of approximated transmittance between 760 and 763 nm for a surface pressure of 1000 hPa and an airmass of 2.41, as a function of the number of eigenvectors used.

AMTD
5, 4473–4494, 2012

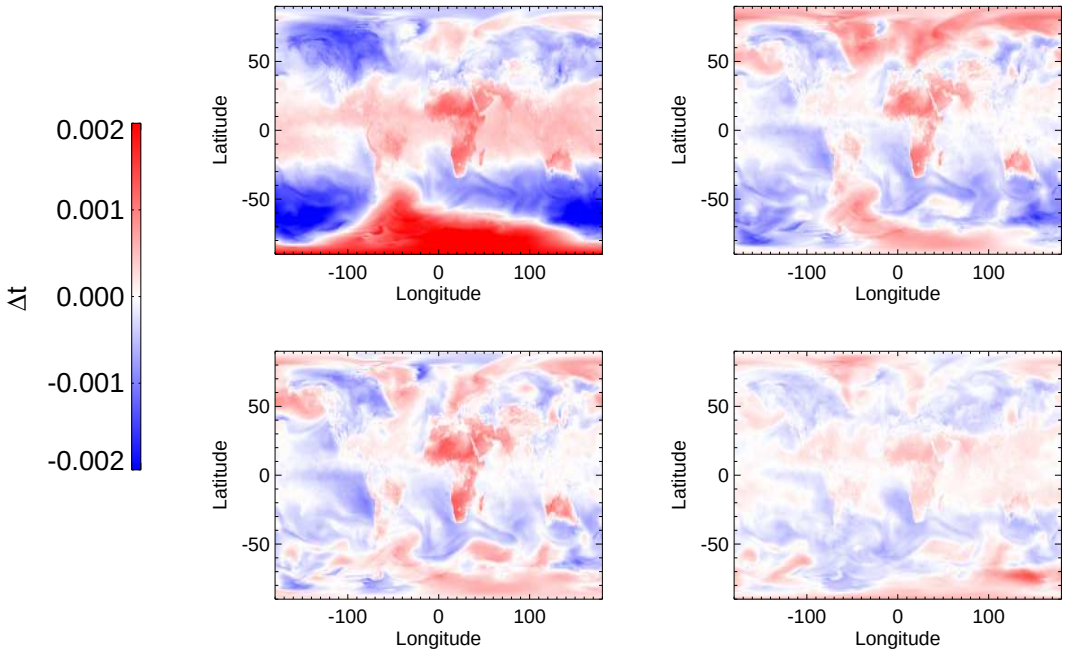

Fig. 5. Global distribution of bias of approximated transmittance $t^*_{O_2A}$, using 1, 2, 3 or 4 eigenvectors (upper left to lower right panels).

AMTD
5, 4473–4494, 2012

On the efficient treatment of temperature profiles

R. Lindstrot and R. Preusker

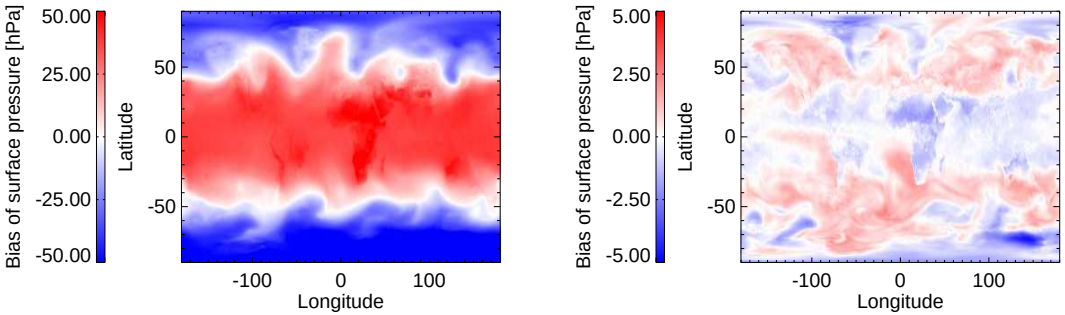

Fig. 6. Global distribution of bias of retrieved surface pressure for a fixed average temperature profile (left panel) and in case four temperature eigenvectors are used for the approximation of the transmittance (right panel), shown for a constant surface pressure of 1000 hPa and an airmass of 2.41. Note the different color bars.

AMTD
5, 4473–4494, 2012

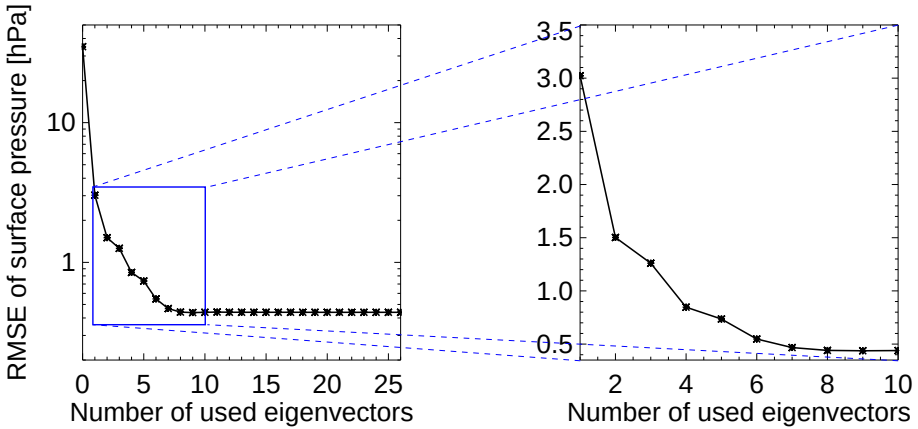

Fig. 7. Global root mean square error of surface pressure, derived from approximated transmittance, as a function of the number of eigenvectors used.

AMTD
5, 4473–4494, 2012

On the efficient treatment of temperature profiles

R. Lindstrot and R. Preusker

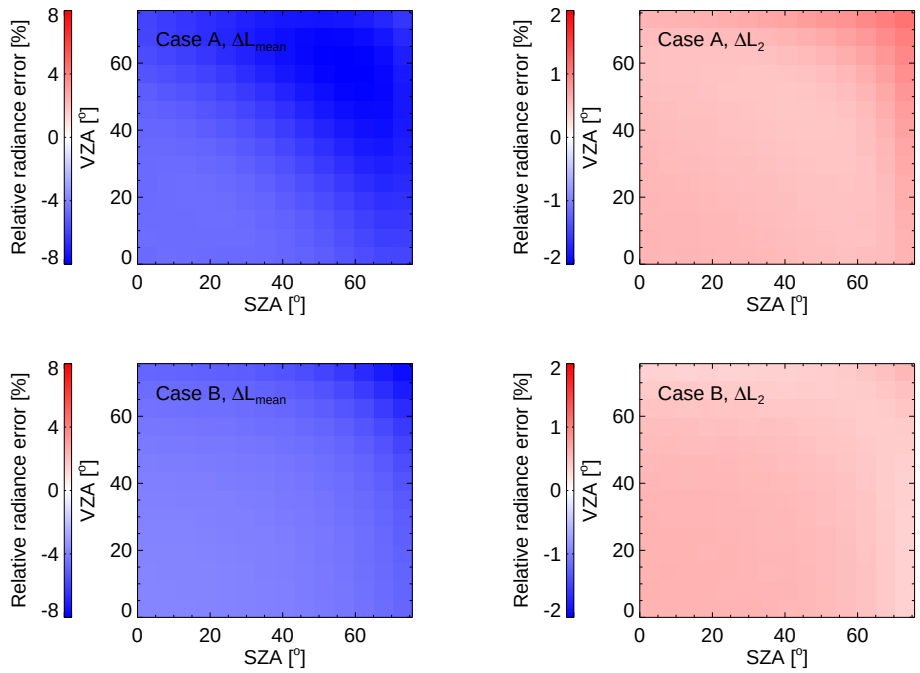

Fig. 8. Angular dependence of error of TOA radiance for the tropical profile for cases A (upper panels) and B (lower panels), a 3 nm-wide channel located at 763 nm and the sensor placed opposite of the sun (relative azimuth angle 0°). Left column shows $\Delta L_{T\text{mean}}$, i.e. the error in case the average profile is used, right column shows ΔL_{v_2}, i.e. the error in case the first two eigenvectors are used. Note the different color bars between both columns.

AMTD
5, 4473–4494, 2012

On the efficient treatment of temperature profiles

R. Lindstrot and R. Preusker

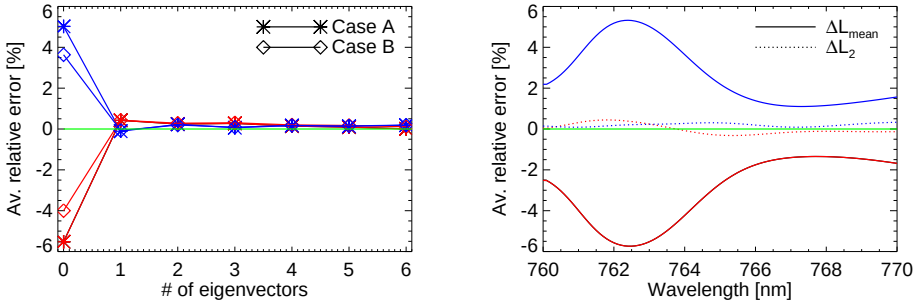

Fig. 9. Left panel: error of approximated radiance (average over all viewing geometries) as a function of number of eigenvectors used, for both cases and both profiles (red lines: tropical profile, blue lines: polar profile) and a spectral channel located at 763 nm. Right panel: error of $L_{T\text{mean}}$ (solid lines) and L_{v_2} (dotted lines) for case A (average over all viewing geometries), as a function of wavelength.

AMTD
5, 4473–4494, 2012

On the efficient treatment of temperature profiles

R. Lindstrot and R. Preusker